Title	Numerical Simulation of Arc and Weld Pool for GTAW in External Axial Magnetic Fields
Author(s)	Yin, Xianqing; Gou, Jianjun; Zhang, Jianxun et al.
Citation	Transactions of JWRI. 2012, WSE2011, p. 17-20
Version Type	VoR
URL	https://doi.org/10.18910/23062
rights	
Note	

Numerical Simulation of Arc and Weld Pool for GTAW in External Axial Magnetic Fields

Xianqing YIN*, Jianjun GOU*, Jianxun ZHANG*, Ninshu MA **

*   School of Material Science and Engineering, Xi'an Jiaotong University, Xi'an 710049, China
**   JWRI, Osaka University, Osaka 567-0047, Japan

KEY WORDS: (Axial Magnetic Field), (GTAW Arc), (Weld Pool), (Fluid Flow), (Numerical Simulation), (Experimental Validation)

1. Introduction

The numerical study on welding is often done in two separate steps, the study on the arc and the study on the weld pool. Many researchers have made a lot of efforts to research the arc [1-4] and the weld pool [5-8], but only several of their models [9-10] contain both of the arc and the pool. So, calculating the arc and the anode at the same time in a integrated model, and the consideration of mutual heat transfer and the force that the arc act on the pool are essential for the research of weld pools.

In external axial magnetic fields, the welding arc is rotated by Lorentz force and thus stirs the pool. This can result grain refinement and better welding quality. The study of the GTAW arc in axial magnetic fields is detailed and complete in document [11], while the pool behavior needs further research. In document [12], the authors consider the influence, to some extent, which is exerted on the pool fluid by axial magnetic field, but they hypothesize that the heat source has a Gaussian distribution and neglect the shear force comes from the arc. These treatments make their results less reliable.

This work is about a complete three-dimensional model for GTA welding in external axial magnetic fields, we focus on the study of how the magnetic field influences the welding behavior, especially the weld pool.

2. Numerical model

The GTAW in external axial magnetic fields is shown schematically in Fig.1. The exciting coil generates the axial magnetic field when it is connected to the power supply. Then the arc is rotated by the Lorentz force and it drives the fluid in the weld pool to rotate. Fig.2 is the three-dimensional computational domain, the radius of the anode is 10mm, the height is 6mm, and the arc length is 3mm. The material of the anode is 1Cr18Ni9Ti, and the inert gas is argon.

Source terms for the arc are the same as document [11]. For the anode, the source term for momentum equations, $S_m = J \times B + \rho \beta g (T - T_0)$, the two terms on the right side of the equation are electromagnetic force and the buoyancy force[5] respectively, where β is the volumetric thermal expansion coefficient, T_0 is the reference temperature.

Table 1 shows boundary conditions for anode. The boundary conditions for other zones are similar to

document [11], while for Area 7, j_{max}= -1.2×10^{8}A/m^2, R_c=0.5 mm in this paper. The physical properties of argon are the same with document [11], and the physical properties of 1Cr18Ni9Ti are taken from document [8].

The calculation steps can be described as follows: First, start the calculation of arc only; when the calculation becomes steady, give Area 3 coupled conditions and initialize the temperature of the anode to 300K to simulate the true condition, and change the Solver from Steady to Unsteady, the time step size is 0.001s, and then start the calculation of the anode and the arc. In this calculation, the Solidification/Melting model is needed.
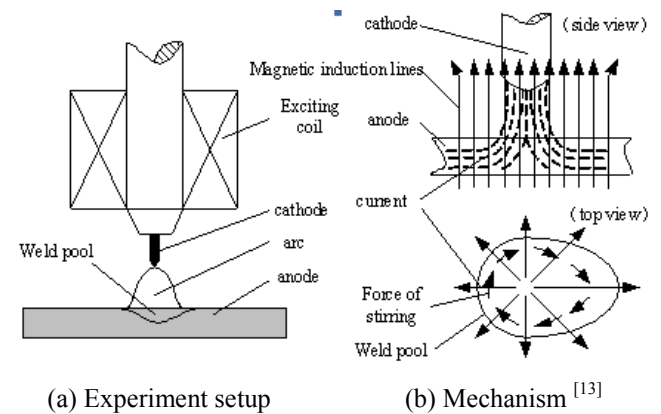

(a) Experiment setup   (b) Mechanism [13]
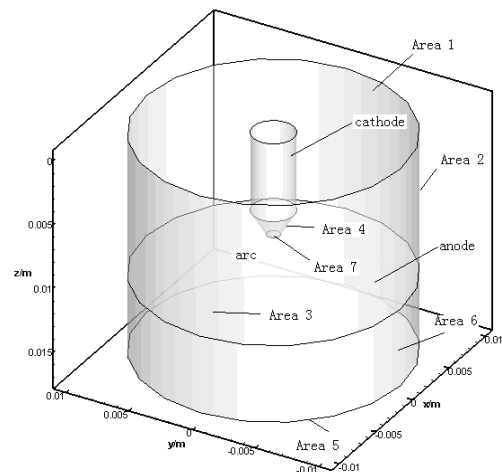
Fig.1 GTAW in external axial magnetic fields

Fig.2 Computational domain

Table 1 Boundary conditions

Boundary	T	P	V	φ	A
Area 3	Coupled	-	-	Coupled	Coupled
Area 5	300 K	-	-	0	-
Area 6	300 K	-	-	$\dfrac{\partial \varphi}{\partial x_i} = 0$	-

3. Results and discussion

3.1 Temperature fields

Fig.3 shows the temperature contour lines of the arc and weld pool in different magnetic fields, the welding time is 2s. In Fig.3 (a), there is no external magnetic field, the welding pool is deeper in the center regions and shallower in the peripheral areas. On the contrary, when an axial magnetic field is applied, things will be totally different. As shown in Fig.3 (b) and (c), weld pools are deeper in edge areas and shallower in center areas. This is because the hot plasma is transported to peripheral areas and the cooler plasma flows back to center areas[11]. As the magnetic induction increases, this trend becomes clearer, and at the same time, the weld pool becomes wider and shallower.
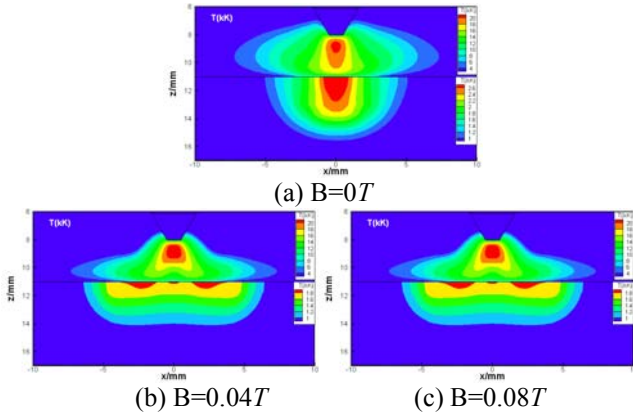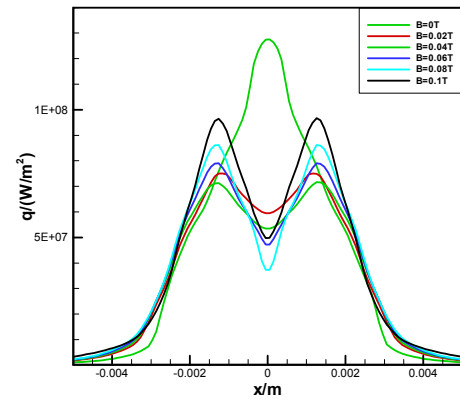

(a) B=0T

(b) B=0.04T (c) B=0.08T

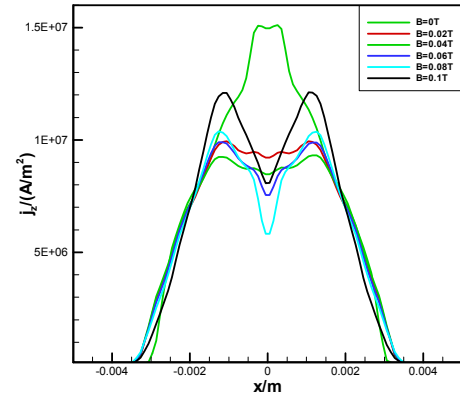Fig.3 Temperature contour line of the arc and weld pool at different magnetic field (t=2s)

Fig.4 shows the distributions of the heat flux and axial current density towards the anode for different magnetic inductions along the radial direction. The heat flux contains radiation heat flux, and the heat due to the conduction and charge motion (q_e). In the arc attachment zone, the flux due to the charge motion is the most important term [4], and q_e is mainly influenced by the axial current density at anode surface, so the heat flux profiles are similar to axial current density profiles.

We have to point out that the current density profile of B=0T is a little abnormal in center areas. There is a flat form between -0.0005 to 0.0005m along x axis, this is because the cathode has a round flat tip, and the current density of the flat tip is a given and relatively high value. And in this situation, the peak value of the current density appears at the edge of the tip. At the same time, the arc length is only 3mm. All these characteristics of the model

make the current density and heat flux at the anode surface have distributions shown in Fig.4 So, we can see that the high platform is in an area of $\pm 0.5mm$, and it is not "very flat" and at the edge of platform the current density is higher than that in center regions.

(a) heat flux

(b) axial current density

Fig.4 Anode heat flux and current density profiles for different magnetic inductions

The current densities at the center of the anode surface for different magnetic inductions are showed in Fig.5. We can see that the computed values approximate to the measured values. The current density at center regions decreases when we strengthened the magnetic field, while the case B=0.1T is a little different. This can be explained by the fact that, to some degree, the high-intensity magnetic field stops the hot plasma's transportation to the periphery of the arc.
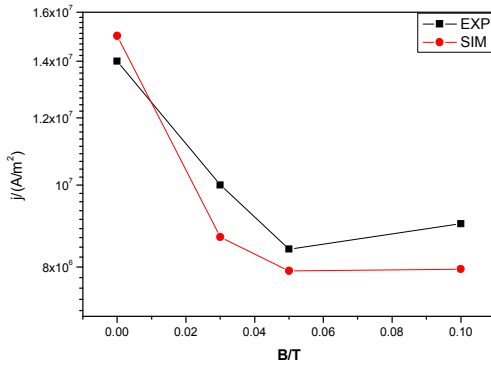
Fig.5 Measured and computed current density

Fig.6 is about the weld width and depth for different magnetic inductions. As shown in the profiles, the weld width increases as the magnetic induction rises, while the weld depth decreases. The weld width increases from 7mm to 11.28mm as the magnetic induction climbs from 0T to 0.1T. On the other hand, the weld depth decreases from 3.75mm to 1.42mm as the induction increases from 0 T to 0.08T. This is because the high-intensity magnetic field enables the bottom of arcs to be extended, and then the heat flux transferred to the anode becomes more dispersed.
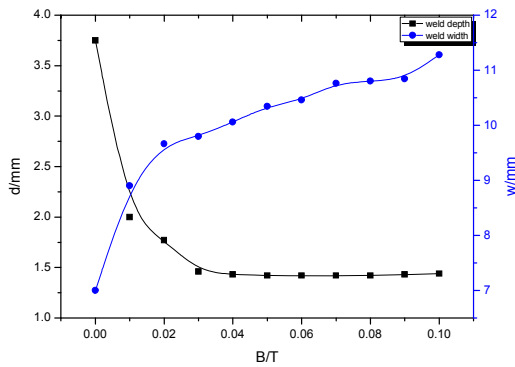

Fig.6 Width and depth of the weld pool (t=2s)

3.2 Velocity fields

Fig.7 is the velocity on the anode surface in different magnetic fields, the view direction is along the +Z axis. Fig.7 (a) is the free arc, the fluid flows inward to the center of the weld pool but the velocity is too small to see when it is compared with other cases. However, in Fig.7 (b) and (c), the fluid in the pool flows outward and rotates clockwise. This is because the arc is rotated by the magnetic field, and the fluid in the pool is rotated by the arc. As the magnetic induction increases, the force generated by the magnetic field becomes larger, and thus the velocity of arc rotation becomes higher and weld pool fluid flows more severely.

In Fig.8, the maximum velocity of rotation of the plasma and the fluid in pool in different magnetic fields are reported. The maximum velocity of the plasma changes from 0 to about 600m/s, while that of the fluid

in the pool increases from 0 to about 0.664 m/s. Both of them are on the rise while the magnetic induction increases. This also can be explained by the larger Lorentz force created by increasing magnetic inductions.

(a) B=0T

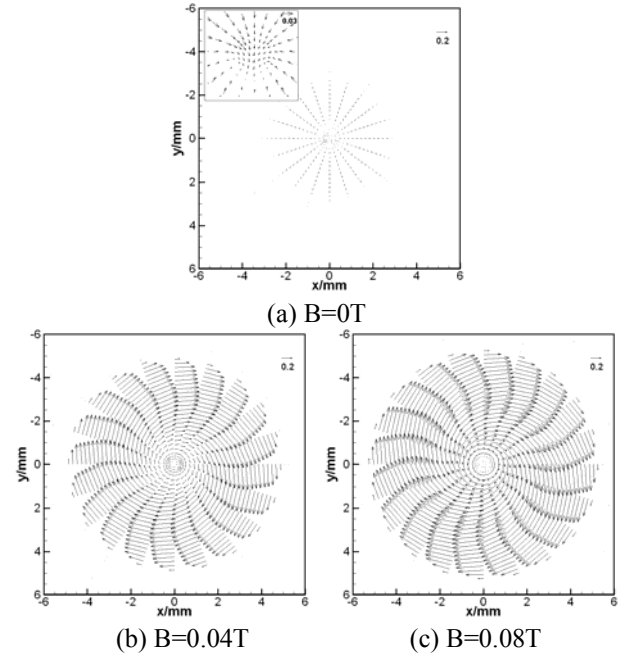(b) B=0.04T   (c) B=0.08T

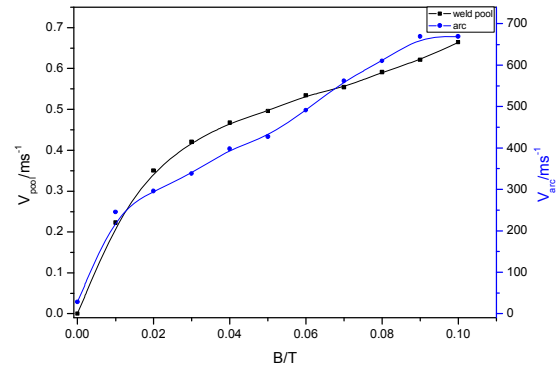Fig.7 Velocity of the anode surface in different magnetic fields (t=2s)

Fig.8 The maximum values of the rotational velocity in different magnetic fields (t=2s)

Fig.9 displays the velocity on the axial cross section of the anode in different magnetic fields. T_l and T_s in Fig.9 (a) indicate the liquids and solidus temperature, respectively. The line T_l represents the bottom outline of the weld pool. When the arc is free, as showed in Fig.9 (a), the fluid flows downward in the arc attachment zone and flows upward in periphery of the weld pool. On the other hand, when the arc is controlled by the magnetic field, in Fig.9 (b) and Fig.9 (c), weld pools are deeper in the two side areas and shallower in the center area. The fluid flows upward in the center area and downward in the edge area, and thus sets up a cycle and enables the weld pool to be shallower in the center area and deeper in the edge area.

On the other hand, when the arc is controlled by the magnetic field, those weld pools are all deeper in the two side area and shallower in the center area. The fluid flows upward in the center area and downward in the edge area, and thus sets up a cycle and enables the weld pool to be shallow in the center area and deep in the edge area. This kind of fluid flow cycle is caused by the decrease of the arc pressure in the center area. Also, as the magnetic induction increases, the arc pressure in the center area becomes negative and the velocity becomes larger, and the weld pool becomes more and more shallower in its center areas.
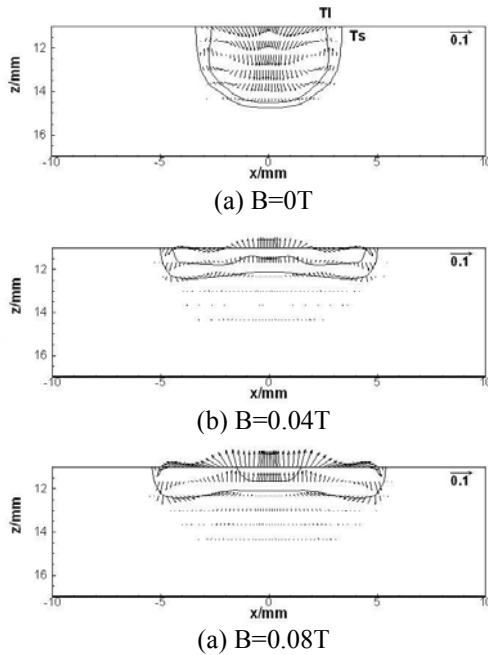

(a) B=0T

(b) B=0.04T

(a) B=0.08T

Fig.9 Velocity on the axial cross section of the anode in different magnetic fields (t=2s).

4. Conclusions

In present paper, a three dimensional numerical model is developed to study the welding arc and weld pool of GTAW in external axial magnetic fields. The welding arc current densities at the center of the anode surface for different magnetic fields are measured and they are similar to the calculated ones.

Under the influence of the external axial magnetic field, the rotated plasmas and the axial magnetic field make the fluid in the molten pool rotate; the arc pressure may become negative in the center area, and this enables the fluid to flow upward in center areas and downward in periphery of the weld pool. Also the heat flux on the anode surface is in a double-peak distribution. All these things make the weld pool become deeper in the peripheral regions and shallower in the center area. As the magnetic induction increases, the weld pool becomes wider, and the width changes from 7mm to 11.28mm, while the depth of the weld decreases to about 1.42mm from 3.75mm.

In this paper, the first step was made towards the study of the relationship between the GTAW arc and molten pool motion behaviors and the external axial magnetic fields parameters.

References

[1] Hus KC, Etemadi K, Pfender E. Study of the free-burning high-intensity argon arc. Journal of Applied Physics, 1983, 54(3): 1293-1301.

[2] Zhu PY, Lowke JJ, Morrow R. A unified theory of free burning arcs, cathode sheaths and cathodes. Journal of Physics D: Applied Physics, 1992, 25: 1221-1230.

[3] Lowke JJ, Morrow R and Haidar J. A simplified unified theory of arcs and their electrodes. Journal of Physics D: Applied Physics, 1997, 30: 2033-2042

[4] R. Bini, M Monno and M I Boulos. Numerical and experimental study of transferred arcs in argon. J.Phys.D:Appl. Phys, 2006, 39: 3253-3266.

[5] T.ZACHARIA, A.H.ERASLAN and D.K. AIDUN. Three-dimensional transient model for arc welding process. Metallurgical transactions B, 1989, 20B: 645-659.

[6] T.ZACHRIA, S.A.DAVID and J.M.VITEK, Computational modeling of stationary gas tungsten arc weld pools and comparison to stainless steel 304 experimental results. Metallurgical transactions B, 1991, 22B: 243-257

[7] H.Purmohamad, A.Kermanpur and M.Shamanian. Numerical simulation and experimental investigation of temperature distribution in the circumferentially butt GTAW of Incoloy 800H pipes. International Journal of Pressure Vessels and Piping, 2010, 87: 424-432.

[8] S.Kou and Y.H. Wang. Three-dimensional convection in laser melted pools. Metallurgical transactions A, 1986, 17A: 2265-2270

[9] M Tanaka, K Yamamoto, S Tashiro. Time-dependent calculations of molten pool formation and thermal plasma with metal vapour in gas tungsten arc welding. Journal of Applied Physics, 2010

[10] Anthony B Murphy. A self-consistent three-dimensional model of the arc, electrode and weld pool in gas-metal arc welding. Journal of Physics D: Applied Physics, 2011

[11] Yin Xianqing, Wu yuanyi, Zhang Jianxun, et al. Numerical analysis of GTAW arc behaviors in external axial magnetic field. International Seminar on Welding Science and Engineering (WSE2011), 17-21 November, 2011, Osaka, Japan

[12] Luo Jian, Zhao Guoji, Wang Xiangjie, et al. Numerical simulation and experimental study of temperature fields for GTAW in external axial magnetic field. Hot working technology, 2010, 39(3): 133-135.

[13] Matsuda F, Nakata K, Miyanaga Y, et al. Effect of Electromagnetic Stirring on Weld Solidification Structure of Aluminum Alloys (Report I): Investigation on GTA Weld Metal of Thin Sheet [J]. Transactions of JWRI, 1978, 7 (1): 111-127.